PHYSICAL REVIEW A, VOLUME 63, 052720

Influence of molecular orientation on the multiple differential cross sections for the $(e,2e)$ process on a water molecule

C. Champion, J. Hanssen, and P. A. Hervieux
Laboratoire de Physique Moléculaire et des Collisions, Institut de Physique, 1 Boulevard Arago, Technopôle 2000, 57078 Metz Cedex 3, France

(Received 17 July 2000; published 19 April 2001)

Eightfold and fivefold differential cross sections (8DCS and 5DCS, respectively) for the $(e,2e)$ process on a water molecule are calculated within the framework of the first Born approximation, and the role of the molecular orientation on the collision process is studied and analyzed. The molecular wave functions are described by the linear combination of atomic orbitals (LCAO) (self-consistent-field LCAO molecular orbitals method). We present results for electron impinging at an intermediate energy of 250 eV and in an asymmetric coplanar geometry and kinematics. When particular molecule orientations are chosen, the 8DCS exhibit large differencies, in shape as well as in magnitude. A comparison of these results with an averaged-space calculation (integration of the 8DCS over Euler angles) confirms the necessity to take properly into account the molecular orientation in the calculations of the ionization cross sections of polyatomic molecules.

DOI: 10.1103/PhysRevA.63.052720 PACS number(s): 34.80.Dp

I. INTRODUCTION

Electron-impact ionization cross sections are widely used in applications such as modeling of fusion plasmas, modeling of radiation effects for both materials and medical research [1,2] and astronomy as well as in basic research in astrophysics [3], atomic, molecular, and plasma physics. There is also a need of numerical data for charged-particle track-structure analysis [4,5], which are the most powerful tools for the understanding of early physical (and even chemical) stages of radiation actions on matter, such as biological samples, for example, which are predominantly constituted by water (about 80% in mass) [6]. In this context, we have developed a theoretical model based on the first Born approximation (FBA) in order to determine $(e,2e)$ multidifferential cross sections. In the energy domain investigated in our work, the FBA is completely justified (see, for example, [7,8] where a detailed study of the different Born approximations can be found). Indeed, the initial state is constituted by an energetic incident particle ($E_i=250$ eV), i.e., with a kinetic energy at least ten times greater than each of the molecular target energy. Concerning the final state, the diffused electron has a kinetic energy E_d greater than 210 eV (i.e., of the same order of the incident energy E_i), i.e., at least 40 times greater than the ejected particle ($E_e=5$ eV). Under these conditions, the initial state can be described as a product of a plane wave function (for the incident electron) with a molecular wave function described by a linear combination of atomic orbitals (LCAO), all centered on the heavy oxygen atom (self-consistent field LCAO molecular orbitals method, [9]). In the final state, the ejected electron is represented by a Coulomb wave function, whereas the scattered electron is described by a plane-wave function.

Moreover, due to the large asymmetry of the collision energies (an ejected energy of $E_e=5$ eV and a diffused energy E_d greater than 210 eV), we do not introduce the exchange effect in the eightfold differential cross section (8DCS) calculations. Indeed, the exchange effect has no influence on the 8DCS in these asymmetric kinematics, and plays an important role only when the ejected velocity matches the diffused one. In the present work, the diffused particle energy is at least equal to 210 eV, leading to a diffused velocity $V_d \gg V_e$ (V_e being the ejected velocity). Moreover as we can see, for example, in [10,11] where the authors present 5DCS calculations for He and H(1s), respectively, the exchange is very negligible even for less asymmetrical kinematic since the first study deals with $E_i=250$ eV and $E_e=50$ eV, whereas the second work deals with $E_i=54.4$ eV and $E_e=5$ eV. However, we have calculated the exchange effect by introducing it in our 8DCS calculations and have found a minor contribution of the order of 1–3 %.

Finally, the molecular orientation is taken into account by introducing the Euler angles in the molecular description. It allows us to study in detail the influence of each molecular orbital on the 8DCS in terms of shape and/or magnitude. In order to determine the relative importance of the molecular orientation on the calculations, we present the 8DCS obtained for an incident energy of 250 eV and an ejected energy of 5 eV in an asymmetric coplanar geometry as functions of the scattered and ejected angles. Moreover, averaged calculations (i.e., 5DCS obtained by integration of the 8DCS over Euler angles) highlight the necessity to take into account the molecular orientation in ionization-cross-section calculations for polyatomic molecules.

In the literature, available theoretical and experimental data concerning the water-molecule ionization remain very scarce. On the experimental side, the most extensive study was performed for an incident energy of 500 eV by Opal *et al.* [12], who measured double differential cross sections in the range of ejected energies $E_e=4.13-205$ eV and ejection angles $\theta_e=30°-180°$. On the theoretical side, the most recent study on the general subject of molecular ionization by electron impact (with a section dedicated to water ionization) was published by Kim and Rudd [13] who developed a ‘‘binary-encounter-dipole model,’’ which combines the

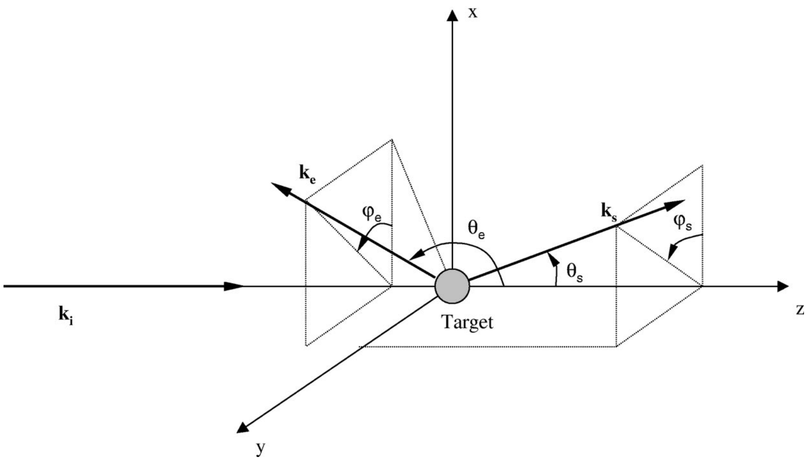

FIG. 1. Reference frame of the ionizing collision of a water target. $\boldsymbol{k}_i$, $\boldsymbol{k}_s$, and $\boldsymbol{k}_e$ represent the wave vectors of the incident, scattered and ejected electrons, respectively. The corresponding polar and azimuthal angles are denoted (θ_s,φ_s) and (θ_e,φ_e), respectively.

binary-encounter theory of Vriens [14] with the dipole interaction of the Bethe theory [15] for fast incident electrons. However, this work gives only a semiclassical description of the ionization process by using average quantities like kinetic energy of the target electrons of each subshell and differential dipole-oscillator strengths for the corresponding molecular orbital. Moreover, these calculations are limited to simple differential and total cross sections. Consequently, the present work appears as a detailed theoretical study of the ionization process of the water molecule by electron impact, and underlines the importance of the molecular orientation during the ionization process. Furthermore, our theoretical approach may be easily introduced in numerical simulations such as Monte Carlo track-structure code for energetic electrons in water [6] or in matter, in general. Indeed for these codes, the multiple differential calculations represent useful input data. Further results concerning the influence of the molecular orientation on the triple, double, and single differential cross sections will be presented in a planned next paper, where theoretical predictions will be compared to available experimental data. The present paper is organized as follows: our theoretical approach is outlined in the Sec. II and the results concerning 8DCS and 5DCS are given and analyzed in the Sec. III. Finally a conclusion is given in Sec. IV. Atomic units are used throughout unless otherwise indicated.

II. THEORETICAL METHOD

In the first Born approximation the nonrelativistic 8DCS is, for a given molecular orientation, defined by the Euler angles $(\alpha;\beta;\gamma)$, and expressed as

$$\left[\frac{d^8\sigma}{d\Omega_s d\Omega_e dE_e d\alpha d\beta d\gamma}\right]_i(\alpha;\beta;\gamma)=\frac{1}{(2\pi)^5}\frac{k_e k_s}{k_i}|T_{if}(\alpha;\beta;\gamma)|^2, \tag{1}$$

where the transition amplitude T_{if} is, without exchange, given by

$$T_{if}(\alpha;\beta;\gamma)=\frac{4\pi}{q^2}|\langle\mathcal{F}^{(-)}_{\mathbf{k}_e}(\mathbf{r})|e^{i\mathbf{q}\cdot\mathbf{r}}|\Psi_i(\mathbf{r})\rangle|^2, \tag{2}$$

where $\boldsymbol{q}=\boldsymbol{k}_i-\boldsymbol{k}_s$ is the momentum transfer (see Fig. 1 for more details).

Ψ_i is the initial wave function of the molecular orbital labeled i and $\mathcal{F}^{(-)}_{\mathbf{k}_e}(\mathbf{r})$ is the Coulomb wave function of ejected momentum $\mathbf{k}_e$ with a charge $z_e=1$. The molecular orbitals are expressed in terms of Slater-like functions all centered at a common origin (the heaviest atom), and are written as

$$\Psi_i(\boldsymbol{r})=\sum_{j=1}^{N_i}a_{ij}\phi^{\xi_{ij}}_{n_{ij}l_{ij}m_{ij}}(\boldsymbol{r}), \tag{3}$$

where N_i is the number of Slater orbitals $\phi^{\xi_{ij}}_{n_{ij}l_{ij}m_{ij}}(\boldsymbol{r})$ and a_{ij} the weight of each atomic component $\phi^{\xi_{ij}}_{n_{ij}l_{ij}m_{ij}}$, the latter being written as

$$\phi^{\xi_{ij}}_{n_{ij}l_{ij}m_{ij}}(\boldsymbol{r})=R^{\xi_{ij}}_{n_{ij}l_{ij}}(r)Y_{l_{ij}m_{ij}}(\hat{r}) \tag{4}$$

with the radial part $R^{\xi_{ij}}_{n_{ij}l_{ij}}(r)$ of each atomic orbital given by

$$R^{\xi_{ij}}_{n_{ij}l_{ij}}(r)=\frac{(2\xi_{ij})^{2n_{ij}+1/2}}{\sqrt{2n_{ij}!}}r^{n_{ij}-1}e^{-\xi_{ij}r}. \tag{5}$$

We have reported in Table I all the parameters (a_{ij},ξ_{ij}) and the quantum numbers (n_{ij},l_{ij},m_{ij}) given by Moccia [9] for the description of the water molecule. The basis sets proposed in this work employed more than 25 functions including, for the spherical harmonics, values of l up to 3. The resulting wave functions refer to the calculated equilibrium configurations, i.e., to the geometrical configurations which, among many others considered, gave the minimum of the total energy and agree very well with the experimental data (see Table II for a summary proposed by Moccia [9]).

For the calculation of the transition amplitude T_{if} [Eq. (2)], we have used the partial wave expansion method. Thus, the continuum Coulomb wave function $\mathcal{F}^{(-)}_{\boldsymbol{k}_e}(\boldsymbol{r})$ and the plane-wave function $e^{i\boldsymbol{q}\cdot\boldsymbol{r}}$ can be written, respectively, as

TABLE I. List of the different coefficients and quantum numbers $(n_{(i)},l_{(i)},m_{(i)})$ included in the linear combination of atomic orbitals for the water molecule description. The five molecular orbitals necessary to describe the water molecule are, respectively, labeled $1A_1$, $2A_1$, $3A_1$, $1B_2$, and $1B_1$. The corresponding ionization potentials are (in atomic units), respectively, 20.5249, 1.3261, 0.5561, 0.6814, and 0.4954.

$n_{(i)}$	$l_{(i)}$	$m_{(i)}$	ξ	$1A_1$	$2A_1$	$3A_1$	$1B_2$	$1B_1$
1	0	0	12.600	0.05167	0.01889	−0.00848		
1	0	0	7.450	0.94656	−0.25592	0.08241		
2	0	0	2.200	−0.01708	0.77745	−0.30752		
2	0	0	3.240	0.02497	0.09939	−0.04132		
2	0	0	1.280	0.00489	0.16359	0.14954		
2	1	0	1.510	0.00107	0.18636	0.79979		
2	1	0	2.440	−0.00244	−0.00835	0.00483		
2	1	0	3.920	0.00275	0.02484	0.24413		
3	2	0	1.600	0.00000	0.00695	0.05935		
3	2	0	2.400	0.00000	0.00215	0.00396		
3	2	2	1.600	−0.00004	−0.06403	−0.09293		
3	2	2	2.400	0.00003	−0.00988	0.01706		
4	3	0	1.950	−0.00004	−0.02628	−0.01929		
4	3	2	1.950	−0.00008	−0.05640	−0.06593		
2	1	−1	1.510				0.88270	
2	1	−1	2.440				−0.07083	
2	1	−1	3.920				0.23189	
3	2	−1	1.600				0.25445	
3	2	−1	2.400				−0.01985	
4	3	−1	1.950				0.04526	
4	3	−3	1.950				−0.06381	
2	1	1	1.510					0.72081
2	1	1	2.440					0.11532
2	1	1	3.920					0.24859
3	2	1	1.600					0.05473
3	2	1	2.400					0.00403
4	3	1	1.950					0.00935
4	3	3	1.950					−0.02691

$$\mathcal{F}^{(-)*}_{\boldsymbol{k}_e}(\boldsymbol{r})=\sum_{l_e=0}^{\infty}\sum_{m_e=-l_e}^{+l_e}(4\pi)(-i)^{l_e}e^{i\sigma_{l_e}}\times\frac{F_{l_e}(k_e;r)}{k_e r}Y_{l_e m_e}(\hat{k}_e)Y^{*}_{l_e m_e}(\hat{r}) \tag{6}$$

TABLE II. Comparison between the calculated values (proposed by Moccia) and the experimental ones concerning the geometrical and energetic properties of the water molecule. The energetic properties concern essentially the electric dipole moment μ and the first Ionization Potential (first IP), whereas the geometrical parameters represent the binding length O-H, the equilibrium distance H-H, and the molecular angle H-O-H.

Water molecule parameter	Calculated value	Experimental value
μ (a.u)	0.8205	0.728
first IP (a.u)	0.4954	0.463
O-H (a.u.)	1.814	1.810
H-H (a.u.)	2.907	2.873
H-O-H	106.53°	105.5°

and

$$e^{i\boldsymbol{q}\cdot\boldsymbol{r}}=\sum_{l=0}^{\infty}\sum_{m=-l}^{+l}(4\pi)i^{l}j_{l}(qr)Y^{*}_{lm}(\hat{q})Y_{lm}(\hat{r}), \tag{7}$$

where the quantum numbers (l_e,m_e) introduced in Eq. (6) correspond to the ejected electron. Moreover, as it is assumed in this work that the ejected electron is moving in a pure Coulomb potential $-1/r$, the Coulomb phase shift is written as

$$\sigma_l=\arg\Gamma(l+1+i\eta_e), \tag{8}$$

where the radial hypergeometric function $F_l(k_e;r)$ is given by

$$F_l(k_e;r)=\frac{1}{2(2l+1)!}\times|\Gamma(l+1+i\eta_e)|e^{-\eta_e\pi/2}(2k_e r)^{l+1}e^{-ik_e r}\times{}_1F_1(l+1-i\eta_e,2l+2,2ik_e r) \tag{9}$$

whose asymptotic behavior is given by

$$F_l(k_e;r) \sim \sin\left[k_e r - l\frac{\pi}{2} - \eta_e \ln(2k_e r) + \sigma_l\right] \tag{10}$$

with $\eta_e = -1/k_e$ being the Sommerfeld parameter. The quantities $j_l(r)$ and $Y_{lm}(\hat{r})$ introduced in Eqs. (6) and (7) correspond to the Bessel functions and the spherical harmonics, respectively.

Taking the direction of the initial momentum $\boldsymbol{k}_i$ to be along the *z* axis (see Fig. 1) we obtain, for the molecular state labeled *i*, the following simplified expression of the 8DCS:

$$\left[\frac{d^8\sigma}{d\Omega_s d\Omega_e dE_e d\alpha d\beta d\gamma}\right]_i (\alpha;\beta;\gamma) = \frac{32}{q^4}\frac{k_s}{k_i k_e}\sum_{j,k=1}^{N_i}\sum_{\mu_j=-l_{ij}}^{+l_{ij}}\sum_{\mu_k=-l_{ik}}^{+l_{ik}} a_{ij}a_{ik}\mathcal{D}^{(l_{ij})}_{\mu_j m_{ij}}(\alpha;\beta;\gamma) \times \mathcal{S}^{\mu_j}_{n_{ij}l_{ij}m_{ij}}[\mathcal{D}^{(l_{ik})}_{\mu_k m_{ik}}(\alpha;\beta;\gamma)\mathcal{S}^{\mu_k}_{n_{ik}l_{ik}m_{ik}}]^*, \tag{11}$$

where N_i is the number of different atomic states included in the molecular state *i* [see Eq. (3)].

$\mathcal{S}^{\mu_j}_{n_{ij}l_{ij}m_{ij}}$ is given by

$$\mathcal{S}^{\mu_j}_{n_{ij}l_{ij}m_{ij}} = \sum_{l_e=0}^{\infty}\sum_{m_e=-l_e}^{+l_e}\sum_{l=0}^{\infty} i^{(l-l_e)}e^{i\sigma_{l_e}}\mathcal{A}^{l_{ij}\mu_j}_{l_e m_e l}\mathcal{R}^{n_{ij}l_{ij}}_{ll_e} \times Y_{l_e m_e}(\hat{k}_e)Y_{l\mu_j-m_e}(\hat{q}), \tag{12}$$

with $\mathcal{A}^{l_{ij}\mu_j}_{l_e m_e l}$ defined by

$$\mathcal{A}^{l_{ij}\mu_j}_{l_e m_e l} = (\hat{l}_{ij}\hat{l}_e\hat{l})^{1/2}\begin{pmatrix} l_{ij} & l_e & l \\ 0 & 0 & 0 \end{pmatrix}\begin{pmatrix} l_{ij} & l_e & l \\ \mu_j & -m_e & m_e-\mu_j \end{pmatrix}, \tag{13}$$

where $\hat{l}_j = (2l_j+1)$, and the radial integration $\mathcal{R}^{n_{ij}l_{ij}}_{ll_e}$ defined by

$$\mathcal{R}^{n_{ij}l_{ij}}_{ll_e} = \int_0^{\infty} R_{n_{ij}l_{ij}}(r)j_l(qr)F_{l_e}(k_e;r)r dr. \tag{14}$$

The angular dependence of the 8DCS given by Eq. (11) is included in the rotation matrix $\mathcal{D}^{(l_j)}_{m_i m_j}(\alpha;\beta;\gamma)$ defined by

$$\mathcal{D}^{(l_j)}_{m_i m_j}(\alpha;\beta;\gamma) = e^{-i\alpha m_i}d^{(l_j)}_{m_i m_j}(\beta)e^{-i\gamma m_j}, \tag{15}$$

where the $d^{(l_j)}_{m_i m_j}(\beta)$ functions are fully determined by the (m_i, m_j, l_j) triplets through the Jacobi polynomials [16,17].

However, in usual experimental conditions, water molecules are not oriented in space. Hence, to compare the measured cross sections to the theoretical predictions, we have to integrate the 8DCS given by Eq. (11) over the Euler angles in order to obtain the 5DCS averaged over all the possible molecular orientations. Then, using the othogonality relation

$$\frac{1}{8\pi^2}\int\int\int \mathcal{D}^{(j_1)}_{m_1 m_1'}(\alpha,\beta,\gamma)\mathcal{D}^{(j_2)*}_{m_2 m_2'}(\alpha,\beta,\gamma) d\alpha d\gamma \sin\beta d\beta = \frac{1}{\hat{j}_1}\delta_{j_1 j_2}\delta_{m_1 m_2}\delta_{m_1' m_2'} \tag{16}$$

it leads to

$$\left[\frac{d^5\sigma}{d\Omega_s d\Omega_e dE_e}\right]_i = \frac{1}{8\pi^2}\int\int\int d\alpha d\gamma \sin\beta d\beta \times \left[\frac{d^8\sigma}{d\Omega_s d\Omega_e dE_e d\alpha d\beta d\gamma}\right]_i (\alpha;\beta;\gamma) = \frac{32}{q^4}\frac{k_s}{k_i k_e}\sum_{j=1}^{N_i}\frac{[a_{ij}]^2}{\hat{l}_{ij}}\sum_{\mu_j=-l_{ij}}^{l_{ij}} |\mathcal{S}^{\mu_j}_{n_{ij}l_{ij}m_{ij}}|^2. \tag{17}$$

Finally, the ‘‘total’’ 8DCS and 5DCS corresponding to the water molecule are given by the summation over the N_{orb} molecular orbitals, where N_{orb} is equal to 5 (see Table I). Hence, we find, respectively,

$$\left[\frac{d^8\sigma}{d\Omega_s d\Omega_e dE_e d\alpha d\beta d\gamma}\right] = \sum_{i=1}^{N_{orb}}\left[\frac{d^8\sigma}{d\Omega_s d\Omega_e dE_e d\alpha d\beta d\gamma}\right]_i (\alpha;\beta;\gamma) = \frac{1}{(2\pi)^5}\frac{k_e k_s}{k_i}\sum_{i=1}^{N_{orb}} |T_{if}(\alpha;\beta;\gamma)|^2 \tag{18}$$

and

$$\left[\frac{d^5\sigma}{d\Omega_s d\Omega_e dE_e}\right] = \sum_{i=1}^{N_{orb}}\left[\frac{d^5\sigma}{d\Omega_s d\Omega_e dE_e}\right]_i = \frac{1}{8\pi^2}\sum_{i=1}^{N_{orb}}\int\int\int d\alpha d\gamma \sin\beta d\beta \times \left[\frac{d^8\sigma}{d\Omega_s d\Omega_e dE_e d\alpha d\beta d\gamma}\right]_i (\alpha;\beta;\gamma) = \frac{32}{q^4}\frac{k_s}{k_i k_e}\sum_{i=1}^{N_{orb}}\sum_{j=1}^{N_i}\frac{[a_{ij}]^2}{\hat{l}_{ij}}\sum_{\mu_j=-l_{ij}}^{l_{ij}} |\mathcal{S}^{\mu_j}_{n_{ij}l_{ij}m_{ij}}|^2. \tag{19}$$

III. RESULTS

The water molecule has the particularity to present a plane symmetry since it is constituted by two hydrogen atoms that are symmetrically sited here and there from the

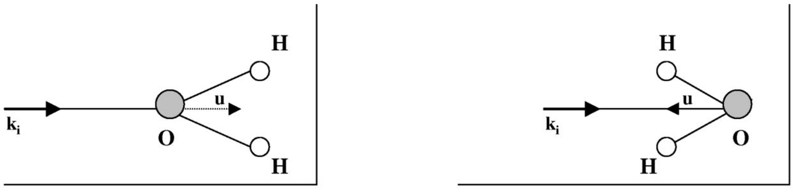

a) Parallel configuration *b) Antiparallel configuration*

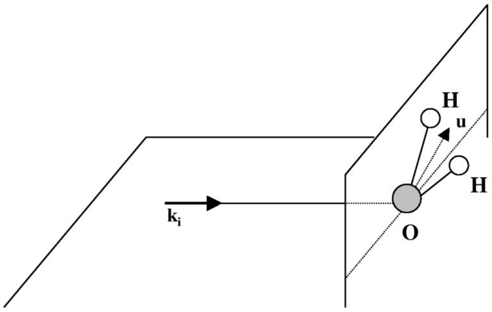

c) Perpendicular configuration

FIG. 2. Schematic representation of the three particular configurations studied in this work. The ‘‘parallel’’ and ‘‘antiparallel’’ configurations correspond to an incident axis $\boldsymbol{k_i}$ in the molecular plane [yz or (HOH) plane]. They differ only by the position of the hydrogen atoms with respect to the incident plane: in the first configuration, the incident electron is first ‘‘perturbed’’ by the oxygen atom whereas in the second one, it is first ‘‘perturbed’’ by the hydrogen atoms.

oxygen atom. Hence, it is possible to define a molecular plane (HOH) whose bissecting line (O$\boldsymbol{u}$) is defined at a 53.27° angle from each of the OH bonds (see Fig. 2 and Table III where the geometrical properties of the water molecule determined by the SCF LCAO MO’s method given by Moccia [9] are reported). In these conditions it appeared pertinent to calculate the 8DCS in three particular molecular orientations. The first one, called the ‘‘parallel configuration’’ [see Fig. 2(a)], corresponding to the case where the O$\boldsymbol{u}$ and the $\boldsymbol{k_i}$ axis are in the same direction and where the incident electron ‘‘encounters,’’ for the first time, the oxygen atom. In the second orientation, called the ‘‘antiparallel configuration’’ [see Fig. 2(b)], the O$\boldsymbol{u}$ and the $\boldsymbol{k_i}$ axis are in opposite directions and the electron beam ‘‘encounters’’ first the H atoms. Finally, the third orientation, called the ‘‘perpendicular configuration’’ [see Fig. 2(c)], is where the molecular plane is oriented at a 90° angle with respect to the incident axis and where the H atoms are sited on the left-hand side. These three molecular orientations correspond, respectively, to the following Euler rotations, all centered on the central oxygen atom: $R_1 = R_O(0°;0°;0°)$, $R_2 = R_O(0°;180°;0°)$, and $R_3 = R_O(0°;90°;90°)$, where the rotation operator $R_O(\alpha;\beta;\gamma)$ is defined by $R_O(\alpha;\beta;\gamma) = R_{Oz''}(\gamma)R_{Oy'}(\beta)R_{Oz}(\gamma)$ [16].

The 8DCS obtained in these different geometrical configurations are presented and discussed in the following section for each molecular orbital and are compared in shape as well as in magnitude in order to enhance the influence of the molecular orientation on the ionizing collision description. Then, we present in the Sec. III B the 8DCS integrated over the Euler angles, i.e., the 5DCS, which permits a better understanding of the geometry influence on the ionizing process. In all cases, we consider the water-molecule ionization by an incident electron of 250 eV with an ejected electron of 5 eV; these energetic conditions justified the use of the FBA approximation. The geometry used corresponds to a coplanar configuration, i.e., $(\varphi_s, \varphi_e) = (0°,0°)$.

TABLE III. Geometrical properties of the equilibrium configuration of the water molecule proposed by Moccia.

Bound length (a.u)	Angular configuration
$R_{\mathrm{OH}} = 1.8140$	symmetry H-O-H=106.53° coplanar geometry: $\phi = 90°$ and $\phi = 270°$

A. Influence of the molecule orientation on the 8DCS calculations

In Figs. 3 and 4, we present the 8DCS calculated for each molecular orbital for two extreme scattered-angle values ($\theta_s = 0°$ and $\theta_s = 15°$), which classically correspond to large and small impact-parameter collisions, respectively. In the first case, the 8DCS will provide useful information about the molecular electronic density of each of the molecular states. In the second case (i.e., for small impact parameter), we will obtain a detailed description of the inner electronic distribution of the water molecule. Moreover, as it will be seen in the following, the overall behavior of these 8DCS’s are essentially dependent on the majority of the atomic components of each molecular orbital (see Table IV). Hence to simplify the discussion, let us first of all underline the different atomic compositions of the molecular orbitals (MO’s), and specially of the four molecular orbitals implicated in the 250 eV collision, i.e., from the first to the fourth MO. As we can see in Table IV, the first MO is predominantly governed by a $2p_{+1}$ atomic orbital, the second MO by a $2p_0$, the third MO by a $2p_{-1}$, and the fourth MO by a $2s$. Then, when we consider the ionization of the water molecule at $\theta_s = 0°$ oriented in the parallel configuration (full line in the Figs. 3), we find that the different molecular orbitals behave like pure atomic orbitals. Hence, concerning the 8DCS for the ‘‘

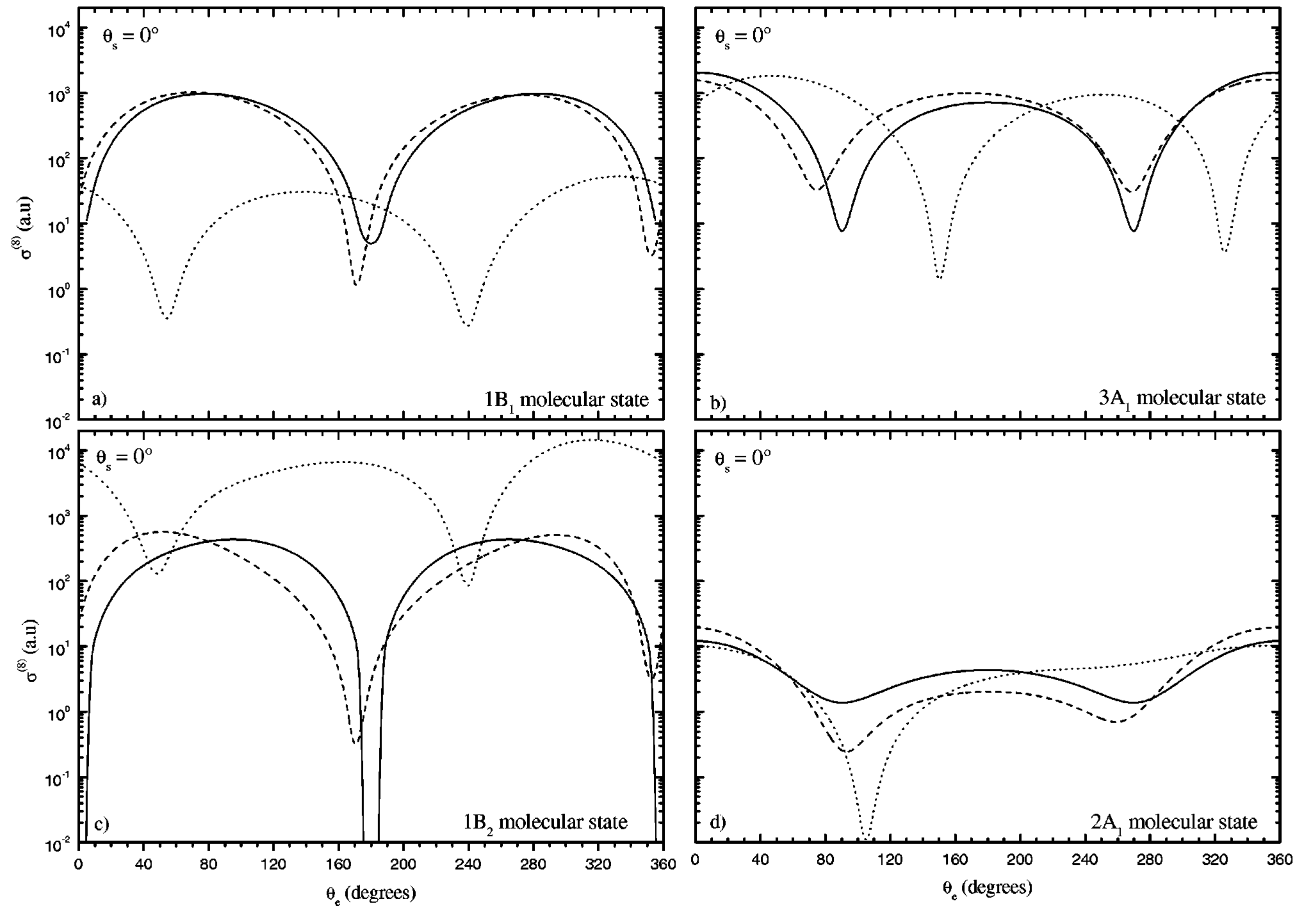

FIG. 3. 8DCS calculated for water-molecule ionization at 250 eV (with an ejected electron of $E_e = 5$ eV), in considering the contribution of each molecular orbital [the figures labeled from (a) to (d) correspond to the first, the second, the third, and the fourth molecular orbital, respectively]. The collision is studied in the coplanar geometry, i.e., $\varphi_e = \varphi_s = 0°$, and with a scattered angle θ_s of 0°. The different molecular orientations studied, denoted "parallel", "antiparallel", and "perpendicular" correspond to $(\alpha;\beta;\gamma) = (0°;0°;0°)$, $(\alpha;\beta;\gamma) = (0°;180°;0°)$, and $(\alpha;\beta;\gamma) = (0°;90°;90°)$, respectively. They are represented by a solid line, a dashed line, and a dotted line, respectively.

$2p_0$-like'' molecular orbital (i.e., the second MO) and for the ''$2p_{\pm 1}$-like'' molecular orbitals (i.e., the first and the third MO), we observe forbidden ejection directions (due to the angular part of the molecular wave function) that appear at 180° from each other. In the ''p_0-like'' case, these minima are found at 90° and 270° whereas they are located at 0° (or 360°) and 180° for the ''$p_{\pm 1}$-like'' molecular states. This behavior is clearly explained by the shape of the charge distribution of the sublevels implied in the collision. Concerning the fourth MO that is essentially governed by a $2s$ atomic sublevel [see Fig. 3(d)], the results obtained exhibit two peaks centered at 180° and 360° that correspond, respectively, to the recoil and the binary peak, this last one being an order of magnitude three greater than the first one. These atomic behaviors are fully described and analyzed in [18] and [11] where the authors presented the 8DCS calculations for hydrogen (H_{2s}, H_{2p_0}, and $H_{2p_{\pm 1}}$) ionization by electron impact.

In summary, at this scattering-angle $\theta_s = 0°$, where the incident electron is sensitive to the whole electronic distribution, we find that the 8DCSs are finally near pure atomic-orbital ones. Moreover, we remark that the three external molecular orbitals have relatively the same contribution to the total molecular 8DCS. However, the fourth MO remains smaller than the others by about a factor of 100 for all the ejected angles. This particularity is not only due to the difference between the ionization potentials, but corresponds specially to the fact that this inner molecular shell is not ''seen'' by the incident electron in this large impact-parameter collision. Hence, the molecular orientation has no influence on the 8DCS calculated for this inner subshell.

When we now consider the antiparallel configuration (dashed line in the Figs. 3), we observe that the calculated 8DCSs remain quasi-identical to the results presented above, in magnitude as well as in shape. The rotation $R_2 = R_O(0°,180°,0°)$ does not significantly perturb the 8DCS and the electronic density seen by the incident electron is, for each molecular orbital, quasi-identical to that seen in the parallel configuration. In fact at this θ_s value the position of the H atoms does not perturb significantly the ionization process, and the discrepancy between the two configurations is not really perceived by the incident particle. Concerning the perpendicular orientation (dotted line in the Figs. 3), the effects of molecule rotation are more important (essentially for

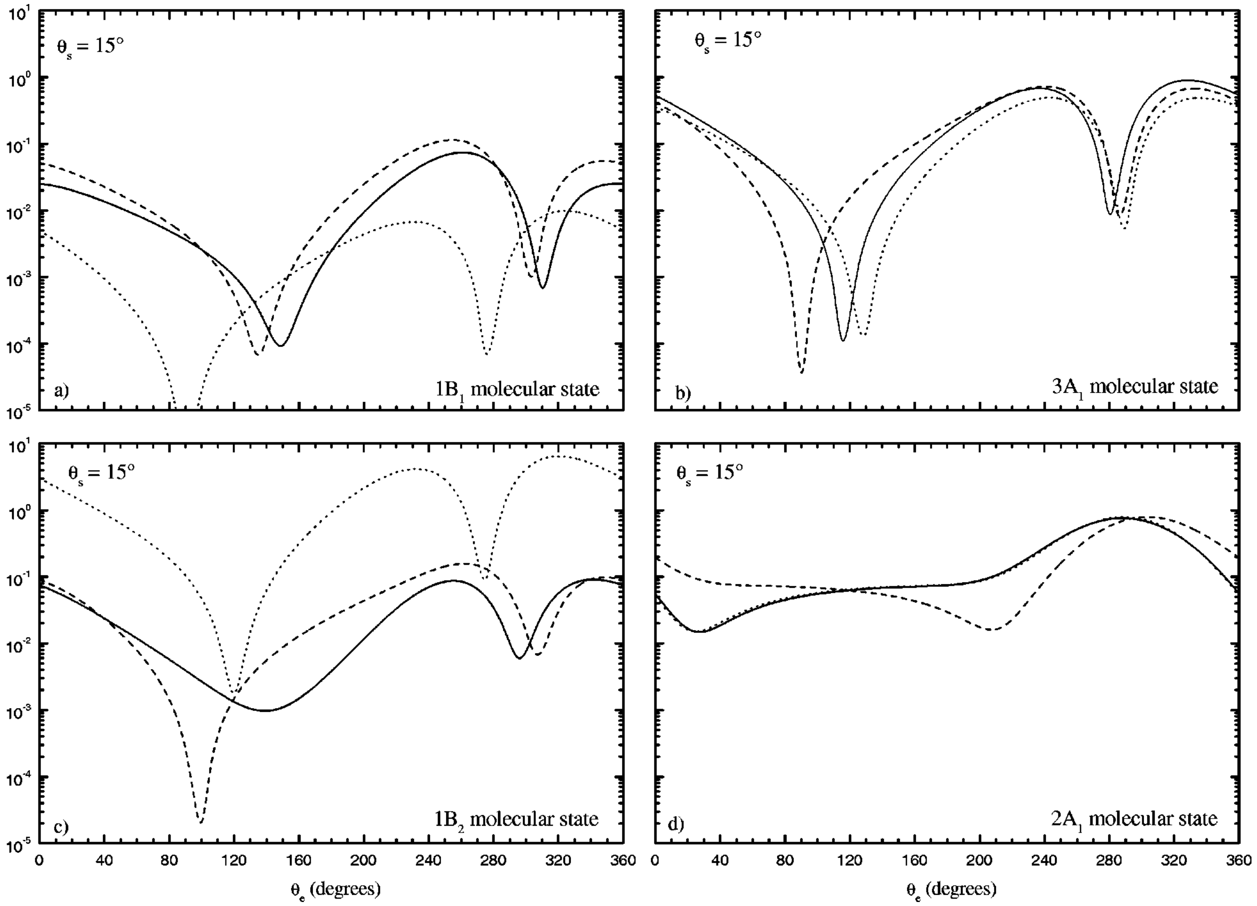

FIG. 4. Same as Fig. 3 with $\theta_s = 15°$.

the three external orbitals since the results for the fourth MO are quasi-identical to these presented above). In fact, for the three outer molecular subshells, the atomic behavior of each of them is inverted and we observe, for instance, that a $2p_{\pm 1}$ orbital behaves, in the perpendicular configuration, as a $2p_0$ orbital and reciprocally, the minima and the maxima are hence found in the same particular directions as those cited above.

Concerning the magnitudes, we observe large discrepancies between the parallel (or antiparallel) results and the perpendicular ones, specially for the first and the third molecular states where we find lesser and greater 8DCSs for the perpendicular configuration, respectively. These particularities are certainly due to the complex atomic combination of these molecular states that can produce interferences between the different atomic subshells, constructive as well as destructive. Indeed, we observe from the Table IV that even these two molecular orbitals exhibit both an overall *p*-like behavior, they present nevertheless large discrepancies in their composition and particulary a non-negligible $3d_{-1}$ component for the third MO. For the other molecular states, the order of magnitude of the 8DCSs remain the same as the 8DCSs obtained for the parallel or antiparallel configurations.

TABLE IV. Dominant atomic orbitals implied in the LCAO of each molecular state of the water molecule. The dominant atomic component is cited first whereas the second one is noted in parentheses.

Molecular state	Dominant atomic component(s)	Ionization potential (a.u.)
$1B_1$	$2p_{+1}$	0.4954
$3A_1$	$2p_0(2s)$	0.5561
$1B_2$	$2p_{-1}(3d_{-1})$	0.6814
$2A_1$	$2s(1s,2p_0)$	1.3261
$1A_1$	$1s$	20.5249

In the same way, we present in Fig. 4 the results obtained in the case of water-molecule ionization at smaller impact parameters (i.e., for larger scattered angles, namely, $\theta_s = 15°$). As a common feature, we observe that the three first molecular orbitals exhibit a p_0-like behavior, i.e., a minimum found for a θ_s value in the direction of the transfer, i.e., a θ_s value of about 270°, which was already observed in the case of hydrogen $(2p_0)$ ionization by electron impact [18]. More precisely, we find that the minima are respectively, localized at $\theta_s = 315°$, 280°, and 300° for the three first molecular states, for the parallel configuration as well as for the antiparallel one. Moreover, the differences observed between the perpendicular configuration and the parallel (or antiparallel) configuration tend to decrease and even disappear [see, for example, Fig. 4(d)].

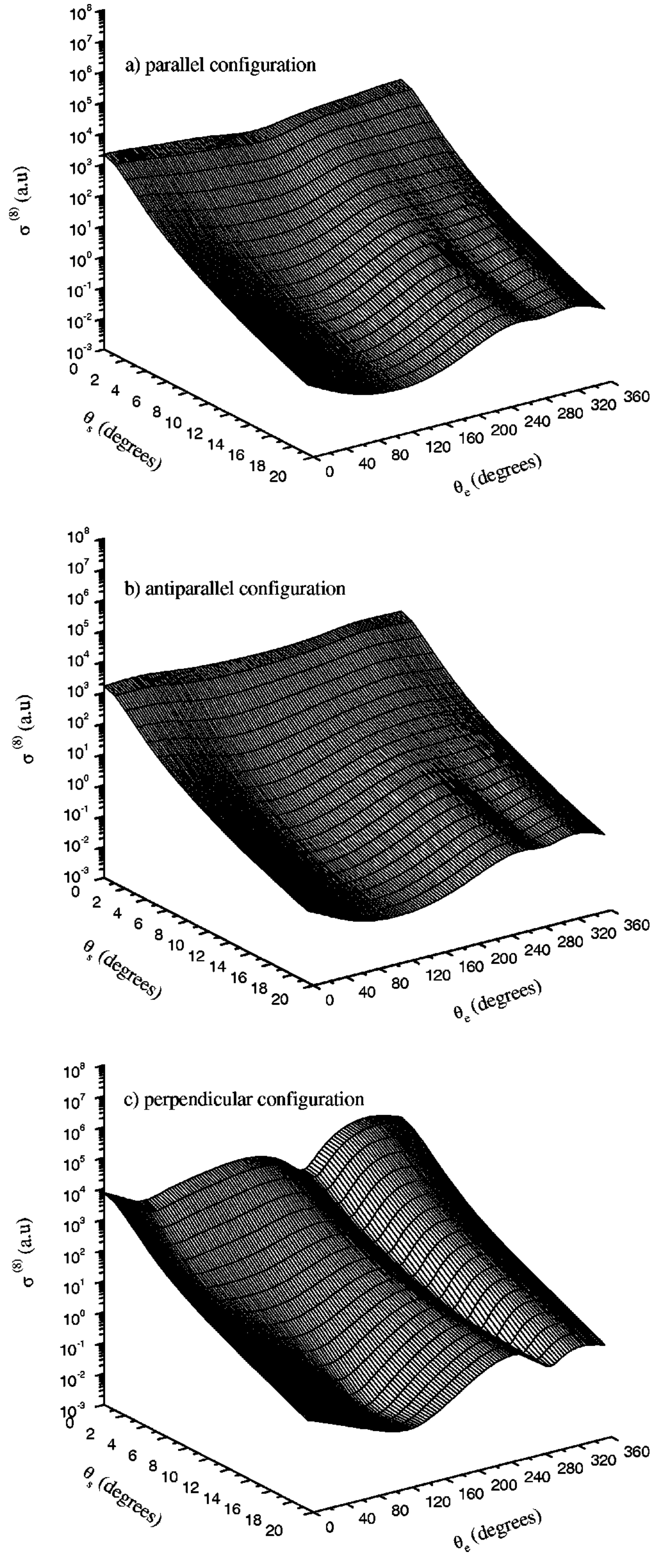

FIG. 5. 3D plots of the ''total'' 8DCS of the water-molecule ionization versus the scattered and ejected angles (θ_s and θ_e) for different molecular orientations: (a) ''parallel configuration'' ($\alpha=0°$; $\beta=0°$; $\gamma=0°$), (b) ''antiparallel configuration'' ($\alpha=0°$; $\beta=180°$; $\gamma=0°$), and (c) ''perpendicular configuration'' ($\alpha=0°$; $\beta=90°$; $\gamma=90°$). In all the figures, the incident energy is 250 eV and the ejected electron has an energy of 5 eV.

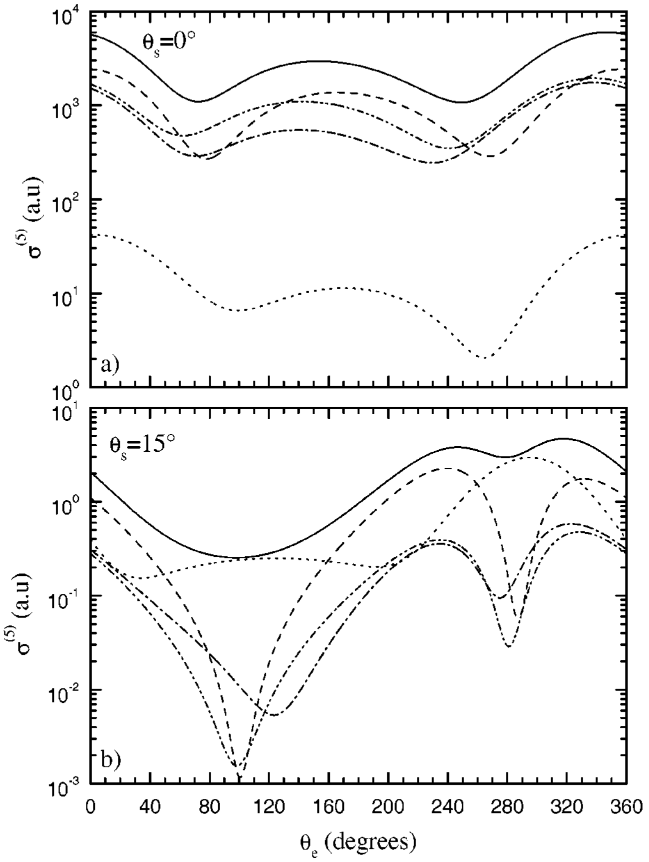

FIG. 6. 5DCS calculated for different scaterred angle values $\theta_s=0°$ (a) and $\theta_s=15°$ (b), respectively. The different subshell contributions are represented: the first MO (dot-dot-and-dashed line), the second MO (dot-and-dashed line), the third MO (dashed line), and the fourth MO (dotted line). The solid line corresponds to the ''total'' 5DCS.

About the orders of magnitude, we observe the same discrepancies between the perpendicular and the parallel (or antiparallel) configuration; the interferences mentioned above could again explain these results. Concerning the fourth MO, we remark that the recoil peak observed in Fig. 3 tends to be negligible, whereas the binary peak centered at $\theta_s=295.07°$ for $\theta_s=15°$ tends to be important, which is in good agreement with the overall behavior of a pure *s* atomic orbital ionized at very small impact parameters. The effect of the rotation of the molecule is finally imperceptible by this inner fourth MO at these scattering angles, and the antiparallel and the perpendicular results tend to be identical [see Fig. 4(d)].

In order to study the influence of molecular orientation on the ''total'' 8DCS, it is interesting to see the variations of the 8DCS versus both the polar angles θ_s and θ_e. We present in Fig. 5 a three-dimensional (3D) plot of the 8DCS for the three molecular orientations studied in this work [Figs. 5(a), 5(b), and 5(c) for the parallel, antiparallel, and perpendicular configurations, respectively]. Hence, we observe at small θ_s values a quasi isotropic distribution for the parallel and the antiparallel orientation whereas it appears a p_0-like behavior for larger values. Hence, when we consider a collision at large impact parameter, the incident electron sees a quasi-spherical electronic distribution, whereas it becomes sensitive to the dominant *p* nature of the water molecule when we consider smaller impact-parameter values. However, concerning the perpendicular-8DCS calculations, we observe more pronounced variations essentially due to the third MO, which exhibits the greater magnitude, as well as for small and for large θ_s values.

B. Angular distribution of the 5DCS (averaged molecular orientation)

When we ionize water molecules in the gas phase, we do not know the real orientation of each molecule in the irradiated volume. In fact, the latter is a random variable, and the molecule can be in any direction. So to compare our 8DCS calculations to experimental results (if they were feasible), it is necessary to average the molecular orientation over the whole solid angle in order to evaluate the 5DCS for ionization of randomly orientated water molecules. Hence, we present in Fig. 6 the results we obtained for two scattering angles ($\theta_s = 0°$ and 15°). Moreover, we plotted the contribution of each molecular subshell in order to evaluate their respective influences on the final result. For large-impact collisions (i.e., $\theta_s = 0°$), we observe that the three outer molecular shells behave like p_0 atomic states, whereas the inner shell exhibits a pure *s* behavior [18]. Hence, the total 5DCS concerning the water molecule presents at this θ_s value, a quasi-p_0 behavior, that is minima for θ_s values of about 90° and 270°. At smaller impact parameters, we observe, like in Fig. 4, that the three outer molecular subshells behave like pure p_0 atomic states in exhibiting forbidden ejection in the transfer direction, namely, at $\theta_s = 280°$. Nevertheless, the total behavior of the water molecule presents a less pronounced p_0 behavior due to the important contribution of the $2s$ molecular state (i.e., the $2A_1$ molecular state) that exhibits a maximum precisely centered at $\theta_s = 280°$ corresponding to the transfer [11].

IV. CONCLUSIONS AND PERSPECTIVES

We have presented in this paper an analytical procedure for the calculation of the 8DCS of the $(e,2e)$ reaction of water-molecule ionization. This approach takes into account the molecular orientation during the collision and allows us to study in detail the influence of the geometrical configuration on the calculations. We have pointed out that the ‘‘total’’ 8DCS could exhibit either ‘‘*s*’’ or ‘‘p_0’’ features versus the particular orientation taken by the molecule. However, when we study the 5DCS variations, i.e., the 8DCS averaged over the Euler angles, we observe a total p_0 behavior, essentially due to the three outer molecular subshells. Hence, this work offers the study of the water-molecule ionization in considering the geometrical point of view for the multiple differential cross section calculations. It is also a step for a complete study of the water-molecule ionization and will be followed by a paper dedicated to the influence of the molecular orientation on the double, simple, and total cross sections.

---

[1] T. A. Tombrello, Nucl. Instrum. Methods Phys. Res. B **2**, 555 (1984).

[2] W. Schimmerling, Radiat. Environ. Biophys. **31**, 197 (1992).

[3] M. Ya Marov, V. I. Shematovich, and D. V. Biscalo, Space Sci. Rev. **76**, 1 (1996).

[4] S. Uehara, H. Nikjoo, and D. T. Goodhead, Phys. Med. Biol. **38**, 1841 (1993).

[5] J. E. Turner, H. G. Paretzke, R. N. Hamm, H. A. Wright, and R. H. Ritchie, Radiat. Res. **92**, 47 (1982).

[6] C. Champion and A. L'Hoir (unpublished).

[7] C. T. Whelan *et al.*, *(e,2e) and Related Processes* (Kluwer Academic, Boston, 1993), pp. 33–74.

[8] I. E. Mc Carthy and E. Weigold, Rep. Prog. Phys. **54**, 789 (1991).

[9] R. Moccia, J. Chem. Phys. **40**, 2186 (1964).

[10] S. Geltman and M. B. Hidalgo, J. Phys. B **7**, 83 (1974).

[11] H. Hafid, B. Joulakian, and C. Dal Cappello, J. Phys. B **26**, 3415 (1993).

[12] C. B. Opal, E. C. Beaty, and W. K. Peterson, At. Data **4**, 209 (1972).

[13] Y-K. Kim and M. E. Rudd, Phys. Rev. A **50**, 3954 (1994).

[14] L. Vriens, *Case Studies in Atomic Physics*, edited by E. W. McDaniel and M. R. C. McDowell (North-Holland, Amsterdam, 1969), Vol. 1, p. 335.

[15] H. Bethe, Ann. Phys. (Leipzig) **5**, 325 (1930).

[16] A. Messiah, *Quantum Mechanics* (North Holland, Amsterdam, 1961), Vol. 2.

[17] L. Landau and E. Lifschitz, *Quantum Mechanics* (Mir, Moscow, 1975), Vol. 3.

[18] J. Hanssen, B. Joulakian, C. Dal Cappello, and H. Hafid, J. Phys. B **27**, 3547 (1994).